Nanotechnology Perceptions
ISSN 1660-6795
www.nano-*ntp.com*

Cfd Modelling And Thermal Distribution Of Solar Assisted Biogas Of Food Waste Towards Renewable Energy

Lemi Negera[1]*, Mahesh Gopal[2]

[1&2] *School of Mechanical Engineering, School of Engineering and Technology, Wollega University,Post Box. No.395, Nekemte, Ethiopia.*
**Correspondence: leminegera574@gmail.com*

This study proposes the Computational Fluid Dynamics (CFD) modelling of a solar-assisted biogas system that utilizes food waste as feedstock. However, climatic temperatures in some places are very low to allow for substantial biogas generation in tiny unheated digesters to fulfill the institute's energy needs, thus the goal is to solve the energy problem using solar panels and a hot water reservoir. In this research, mathematical modeling of the biogas digester and analysis of the losses were calculated. The Flat Plate collector (FPC) of $2m^2$ and cylindrical fixed dome digester of 4.905m diameter and 2m height are designed to heat water to heat food waste. A CFD technique was used to investigate the effect of water mass flow rate of 0.01-0.05 kg/s on the collector's flat plate results the temperature increase, pressure drop, and velocity, as well as the change in flow type intensity. The optimal temperature for this process was 37 ± 2°C. Furthermore, the temperature in the digester dome was properly predicted using CFD modeling. The resulting results have been verified using analytical results. This study helps to generate novel solutions for a more sustainable future by utilizing computational methods to maximize system performance and environmental effects.

Keywords: Anaerobic fermentation; Biogas; Digester; Flat plate collector; Solar water heater.

1. Introduction

The introduction should briefly place the study in a broad context and define the purpose of the work and its significance. Anaerobic digestion is a particularly promising approach for agricultural waste management, as it prevents contamination while also producing energy efficiently. McGrath and Mason (2004) [1] investigated the alternative approach to estimating the biogas output from anaerobic ponds from farm dairy wastewater. The investigation was carried out by Hansen et al. (2007) [2] using 55 samples of pre-treated source-sorted urban organic waste, which is critical for the quantity of biomass that may be routed to a digester. This paper proposes a decision-making kit for the economic assessment of biogas anaerobic digestion designs employing agricultural feedstocks Karellas et al. (2010) [3]. The author, Xydis et al. (2013) [4], carried out a study effort to investigate energetically the electricity generation from a landfill and explored how the expansion of the landfill affects electricity production. The single / two-stage batch digestion method was outperformed by Jeihanipour

et al. (2013) [5] to generate biogas using cotton/polyester and viscose/polyester. The three-part experimental investigation was done by Lee et al. (2013) [6] using biogas with 73% methane content. The influence of the biogas supply rate is discussed first, followed by the study done on biogas with 60% methane content. Finally, with a 73% methane concentration, biogas is examined using a waste-heat recovery system. Ngumah et al. (2013) [7] investigated using waste from animals, human feces, residue from crops, and municipality solid waste using anaerobic digestion. The investigation was done to study the animal wastes, people manure, residue from crops, and municipal solid waste for the biogas harvest using anaerobic digestion Ngumah et al. (2013) [8]. A review analysis of CFD modeling and simulation was done by Farid et al. (2025) [9] for anaerobic digestion reactors used to generate energy from organic waste, Panchenko et al. (2023) [10] reviewed harnessing solar energy in the operation of anaerobic digestion systems, Rodríguez-Jiménez et al. (2022) [11] reviewed solutions for improving anaerobic digestion of food waste at psychrophilic temperatures. The authors Servati and Hajinezhad (2020) [12]used CFD simulations to study the impact of sludge rheology on mixing, flow dynamics, and biogas production in an anaerobic digester and found that increasing the blending speed until the velocity gradient approaches this range improves biogas production. The hydrodynamic behavior of gas-lift and mechanical mixing digesters was explored using two-phase liquid and gas modeling with CFD, which optimizes the anaerobic digester design, velocity field, dynamic viscosity, and ideal mixing type Chen et al. (2019) [13]. The gas-mixed high solids anaerobic digestion (HS-AD) system was analyzed by Li et al. (2022) [14] using CFD modeling to maximize the mixing performance of gas and non-Newtonian fluids. The analysis was done by mixing process and calculated the overall energy consumption required for stirring using an asymmetrical mixer to assess the creation of stagnated volume and the gradient of velocity in the digester Dabiri et al. (2021) [15]. Li et al. (2023) [16] developed a solar-powered water heater and anaerobic digestion system with effective temperature control, demonstrating the viability of a yearly biogas generation system operated with solar energy.

The aforementioned review literature did not address the design and CFD modeling of a solar-assisted biogas system that produces biogas from food waste by designing a solar water heater to heat the digester system. This study proposes a novel CFD framework for assessing solar-assisted anaerobic digestion, which provides new insights into renewable energy efficiency, heat usage, and biogas optimization. The discoveries advance sustainable waste-to-energy solutions, having a substantial influence on green energy and bio-resource engineering.

2. Biogas Digester

2.1. Design of Digester

The anaerobic digester's size was decided using the quantity of waste food per day, the time frame for retention, and the digester's capacity Dewangan and Mishra (2016) [9].

$$\text{Size of a digester } (m^3) = \text{Daily feed intake } (m^3/\text{day}) \times \text{Retention time (day)} \quad (1)$$

$$\text{The total digester volume} = V_t = V_{gc} + V_{gs} + V_{fc} + V_{sl} \quad (2)$$

Where, V_{gc}: gas collection container volume, V_{gs}: gas storage container volume, V_{fc}: fermenting container volume, V_H: hydraulic container volume, V_{sl}: sludge layer volume. The Geometrical dimension of the digester Asmare (2014) [10].

The overall volume (V_o) = $V_{gc} + V_{gs} + V_m + V_b = V_t + V_m + V_b$, $V_t = V_{gc} + V_{gs}$
(3)
Where, Gas storage container volume (V_{gs}) = $V_{gc} + V_{gs}$, Fermentation container volume (V_{fc}) = V_b,
Volume of Sludge layer V_m, $V_m + V_b$ (volume of slurry), The digester's upper and lower radii = R_1 and R_2. Surface area of the top and bottom domes = S_2 and S_2, Maximum distance among the top and bottom domes = f_1 and f_2. The volume of the digester was taken as per the suggestion given by Tadesse and Adamu (2017) [11].

$$V_{gc} \leq 5\% V \quad (4)$$

$$V_s \leq 15\% V \quad (5)$$

$$+V_f = 80\%V \quad (6)$$

$$V_{gs} = VH \quad (7)$$

$$V_{gs} = 0.5 \left(V_{gs} + V_f + V_s\right)K \quad (8)$$

K = 0.3 is the gas output rate per m^3 digester capacity per day.

Geometric measurements of the digester proposed by Asmare (2014) (10)

$$D_d = 1.3078 \times Vo^{1/3} \quad (9)$$

$$V_t = 0.0827\, {D_d}^3, V_m = 0.05011\, {D_d}^3\ V_b = 0.3142\, {D_d}^3 \quad (10)$$

$$R_t = 0.725\, D_d, R_b = 1.0625\, D_d \quad (11)$$

$$f_1 = {D_d}/{5}\ , f_2 = {D_d}/{8} \quad (12)$$

$$S_1 = 0.911\, {D_d}^2, S_2 = 0.8345\, D_d \quad (13)$$

Where, D_d - digester diameter, V_t, V_m, V_b – digester volume of top, middle and bottom.
The density of food particles is 1160 kg/m^3. The water percentage of food trash is 70%. The organic composition of food waste is 85%. Mesophilic temp is 35°. The average solid content is 8%. Time for retention = 45 days. The energy concentration in biogas is 38 MJ/m^3, and specific gas production is 0.04 m^3/kg.

The volume of the daily charge

$$s_d = \frac{\text{Total mass of biodegradable waste}}{\text{The density of food waste}} = 0.964 m^3 day \quad (14)$$

When the waste product is moist, the one-to-one diluting ratio is employed to achieve the required solid content of 8 percent, which corresponds to 0.964m^3 of water every day. As a result, the daily charge volume (S_d) is 1.927586 cubic meters.

The digester volume (V_D) is determined by multiplying the daily charging volume (S_d) by the hydraulic retention time (period). Digester volume =

$$\frac{\text{Cumulative waste per day} * \text{retention period}}{\text{the density of waste in one time frame for retention}}$$

Let hydraulic retention period = 45days, $V_{dD} = S_d \times HRT = 87\ m^3$ (15)

The tank volume (V_D) is set at 43.5m^3 for two digesters to reduce the danger of damage. The dimensions of the mixing pit should be slightly larger than the daily inflow, and it is preferable if there are no corners Asmare (2014) [10]. Let d is the diameter and h is the height of the mixing pit be equal.

$V_t = \frac{\pi d^2 h}{4}$ Vt= 10% × 1.92586m^2/day + 1.925586m^2/day = =2.118446m^3/day (16)

Vt represents the daily substrate mobility of trash after applying a 10 percent factor of safety.

$d = \frac{(2.118446 \times 4)^{1/3}}{3.14} = 1.392\text{m}, \text{Mixing height (h)}, (d) = 1.392\text{m}.$ (17)

The compensation tank (V_{ta}) is around 20% of the total volume of the digester.

V_{ta} = 0.200 × 43.5m^3 = 8.7m^3 for effective space.

Consider a cubic shape of length 'a'.

V= a × a × a = a3, this means a=$\sqrt[3]{V_{ta}}$ =$\sqrt[3]{8.7}$ = 2.0567m^3

To determine the volume of the digestive chamber = digester Volume (V_D) = (V_b+V_m)

Implies $D = \sqrt[3]{\frac{43.5}{0.36431}} = 4.905\text{m}$ (18)

V_t = 9.709m^3, V_m = 5.91m^3, V_b = 37.0786m^3

$\text{The total volume of the chamber } (V) = V_t + V_m + V_b == 52.6976m^3$ (19)

$V_{gs} = VH = k\,(V_m + V_b)/\,(1 - 0.5k) = 7.8095m^3$ (20)

$V_b = \frac{\pi D^2 H}{4} = H = 1.965m$ (21)

The results are derived using the following equation to construct the primary dimension of the digester depending on the values of D and H.

Table1. The dimensions of the digester's primary components

Sl.No	Main Parameters calculated	Results of dimensions
1	D	4.905m
2	H	1.965 m
3	f_1	0.981m
4	f_2	0.612m
5	S_1	21.92m^2

6	S_2	20.1m^2
7	V_{gc}	2.64m^3
8	V_{sl}	7.91m^3
9	R_t	3.56m
10	R_b	5.212m
11	V	52.7m^3

To calculate the warm water storage tank capacity, estimate every day's hot water demand and select the storage tank volume. It should be around 0.8 to 1.2 times the daily demand for areas with strong solar radiation and 2 to 2.5 times the daily requirement for regions with low solar radiation, respectively, so the consuming peaks can be met effectively and overcast days may be compensated.

$$V_{st} = THWD \times 1.2 \quad = 22.041m^3 \quad (22)$$

The collecting tubes have a uniform mass flow rate

$$\dot{m}f = \frac{mhw}{n} \quad (23)$$

The hot water requirement is determined by how much hot water the digester consumes. The water storage unit's energy storage capacity at constant temperature is determined by:

$$Q_s = \dot{m}\, c_p \Delta T \quad = 3702.888 \text{ KWh} \quad (24)$$

Where: Q_s = Storage tank total heat capacity (Kwh) $\dot{m}$ = Storage tank volume (m^3), c_p = 4.2 KWh/m^3. K, ΔT = Difference in temperature → hot and cold water temperature (K).

2.2. Storage tank volume

When the average daily demand for warm water has been assessed, the tank's volume can be determined. The storage tank capacity (V_{st}) should be 0.8 to 1.2 times the amount of water needed every day in areas with high solar radiation, and 2 to 2.5 times the daily need in areas with low solar radiation.

$$V_{st} = THWS \times 1.2 \quad (25)$$

For Jimma town's climatic circumstances, a single collector's storage tank volume is assumed to be 0.125 m^3, and its daily heating capacity is assumed to be 0.15 m^3/day Alemu (1998) [12]. Thus, the size of the storage container required to heat the entire everyday use of hot water is:

$$\text{Total storage tank volume} = \text{The amount of hot water consumed each day} \times \frac{\text{The approximated volume of a storage container for 1 collector}}{\text{The estimated amount of water heated by 1 collector every day}} \quad (26)$$

The estimated amount of water heated by 1 collector every day. Two storage tanks, each having a capacity of 7.7 m^3, are required. The hot water enters the tank from the top and exits via the bottom. The outside walls are insulated.

2.3. Diameter and Height of the Storage Tank

The storage tanks are circular cylinders with a 2:1 height-to-diameter ratio. The diameter and height of the thermal storage tank were determined using the anaerobic digester's daily and

weekly hot water consumption trends. For an annular cylinder with a height-to-diameter ratio equal to 2:1, the storage tank height is given as

$$h = 2 \times Di \quad (27)$$

The volume of one storage tank has been arranged as follows =

$$V_s = \frac{\pi Di^2}{4} \times h = \frac{\pi Di^3}{2} \quad (28)$$

From equation 28, the storage tank's inner diameter is:

$$D_i = \sqrt[3]{\frac{2 \times Vs}{\pi}} \quad (29)$$

2.4. Storage Tank Surface Area

The overall area of the storage tank is calculated by

$$A_s = \pi Dih + 2 \times \left(\frac{\pi Di^2}{4}\right) \quad (30)$$

Table 2. The dimensions of the digester's primary components

Sl.No	Main Parameters calculated	Results of dimensions
1	Volume of the storage tank (V_{st})	22041 liter or 22.041m^3
2	Total volume of storage tank	15.307m^3 for Jimma zone climate
3	Diameter of the (Di)	1.7m
4	Height of storage tank	3.44m
5	Overall area of the storage tank	22.7m^2

3. CFD simulation of anaerobic digester

The computational fluid dynamics (CFD) analysis of the system begins with the development of the desired shape and mesh for modeling the domain. The current investigation made use of a different version of the Ansys Fluent software. In this model, the solid particles and liquid phase are treated as a single homogenous phase with the same density and viscosity as the solid-liquid combination. Homogenous and its behavior are remarkably similar to that of a single-phase mixture. The essential flow equations employed include viscous fluxes in laminar and turbulent flow, as well as the momentum equation in discrete form. The magnitudes of velocity, pressure, and temperature are estimated discretely at the nodes of a mesh or network to describe flow geometry modeling.

3.1. Solver

3.1.1. Boundary conditions

The mass flow inflow boundary condition was applied. The outflow was the pressure outlet; the remainder of the geometry is represented by wall boundary conditions; and finally, the helical coil boundary conditions are the hot water domain. Turbulent flow using the usual k-ε model. After defining the model settings, multiple iterations were undertaken to determine the

mass flow rate. A continuous fluid's physical parameters include density (1200 kg/m^3) and dynamic viscosity (0.02 Pa-s). The simple method is used to couple pressure and velocity. Discretization is accomplished using the second-order upwind approach.

3.1.2. Post-processing

The simulation examines the results with the help of contours, vectors, plots, and other possible ways. Next step, in this digester dome the line in different axis to draw the graphs of the temperature distribution.

3.2. Model the geometry:

The Computational fluid dynamics (CFD) geometry of the dome digester and helical coil type heat exchanger are shown in Figure 1.

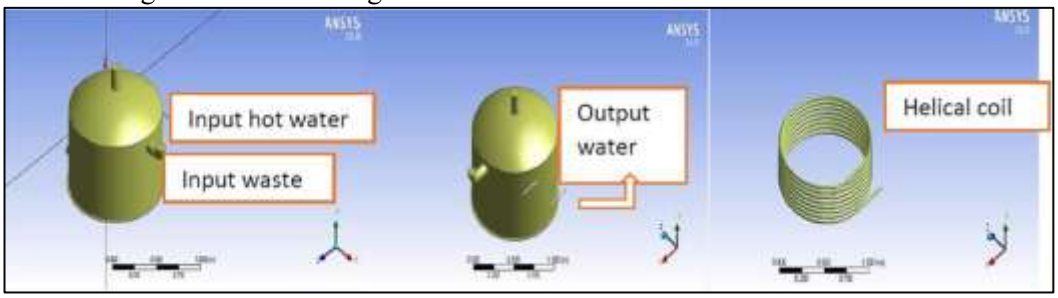

Figure 1. Model of Fixed Dome Digester

3.3. Mesh

Meshing is the process of discretizing the domain into tiny volumes and solving equations using iterative approaches. A mathematical model is constructed from the geometric model, known as meshing or discretization of the continuum, which results in a system of equations. Several simplifications were performed to improve the model's relationship with CFD. These meshes differ in terms of the generation technique, time involved, density, and quality. Various meshing procedures are used with the pre-processor. Figure 2 shows the fine mesh type fixed dome & section view mesh of the digester, Table 3 shows the mesh I information of the biogas digester and Figure 3 shows the meshed digester visible view & helical coil meshed view.

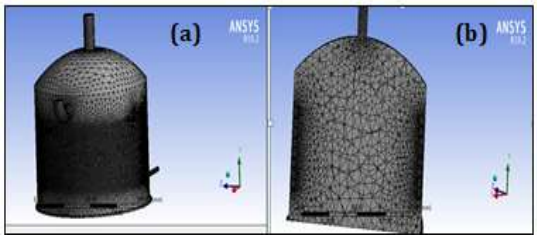

Figure 2. (a) (b) Fine mesh type fixed dome section mesh of digester visible

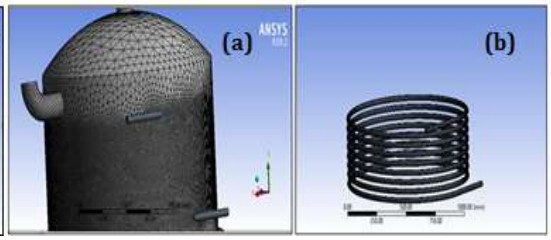

Figure 3. (a) Meshed digester visible view (b) helical coil meshed view

Table 3. Mesh information of biogas digester

Type	Nodes	Element

Fluid coil	967488	831380
Helical coil	635668	346704
Shell tank	21911	107068
All domains	1625067	1285152

4. Results and Discussion

Figure 4 depicts the short-term variations of the analytical and CFD simulations for the identical mass flow rate and material used in the design.

4.1. CFD Simulations of Fixed Dome Anaerobic Digesters

This work presents a three-dimensional steady-state CFD simulation of a specific anaerobic digester to visualize flow patterns and heat transmission. This simulation was performed to determine the heat transfer of hot water with waste food in the digester via the helical coil and food particles in the fixed dome digester. Velocity, pressure, and temperature magnitudes are computed discretely at the mesh nodes to describe flow geometry modeling Mohammadrezaei et al. (2017) [13].

4.2. Pressure contour in all fixed dome digesters

Figure 4 shows the pressure drop in the digester in different ways. Figure 5 depicts the downward fluctuation in pressure in all components owing to heat transfer from hot water to waste material in the digester.

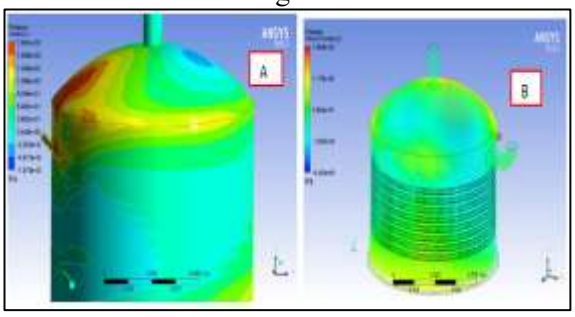

Figure 4. (a) Pressure contours of the entire dome Digesters (b)Pressure volume rendering

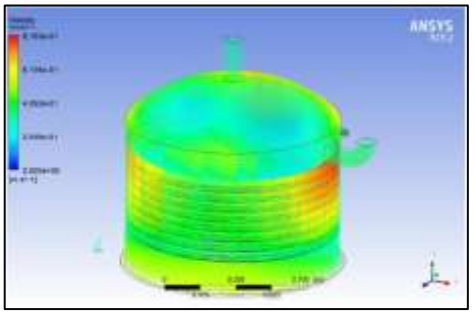

Figure 5. Velocity vector &Velocity contours in the spiral type

4.3. Velocity contour in the dome digester

Velocity is thought to be a better indicator of flow behavior. The velocity of food waste within the digester and the temperature of water inside the coil were determined. Figure 6 depicts the velocity field region of the interior digester and center helical pipe. The hue blue signifies lesser velocities, whereas red represents the highest values. The greatest velocity was 0.82 m/s.

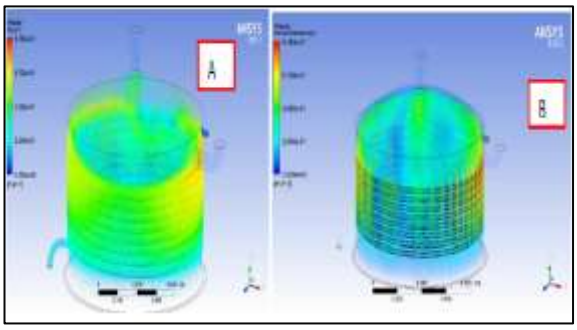

Figure 6. (a)Velocity vector of waste food (b) Velocity volume rendering

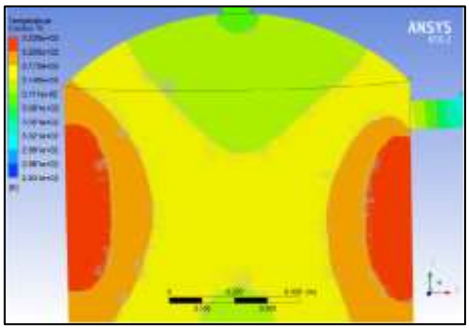

Figure 7. Temperature contour at the plane selection in the dome

4.4. Temperature distribution in the fixed dome heat exchanger

Figure 7 reveals that the average outflow temperature was 310K, which causes a color variation in the digester dome, due to the variation in temperature between hot water and waste material in the digester. Generally, from the simulation of the fermentation tank the average inlet/outlet temperature of the fermentation tank was 323 to 302K. The temperature was varied also in different plane selections in the digester as shown in Figure 8. The temperature was high in the wall and transferred from the hot water temperature from the helical coil to the waste food. Figure 9 illustrates the temperature distribution in the different plane selections. The temperature was high at the wall of the dome and decreased in the center due to the coil being attached to the wall of the digester. The average temperature distribution in this plane was 317K

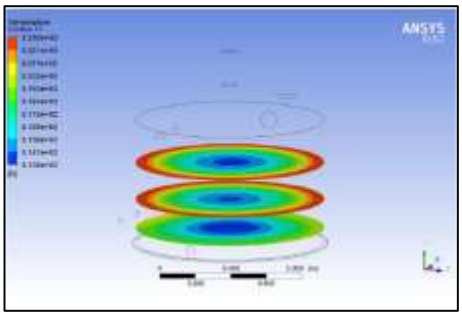

Figure 8. Temperature distribution along the dome in the plane selection

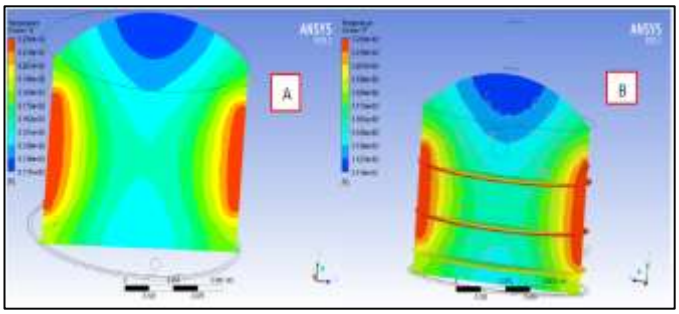

Figure 9. (a) Temperature distribution at the different plane in the vertical (b) in both plane

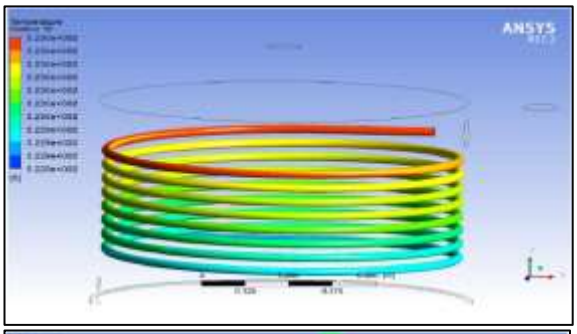

Figure 10. Temperature contour in the helical coil

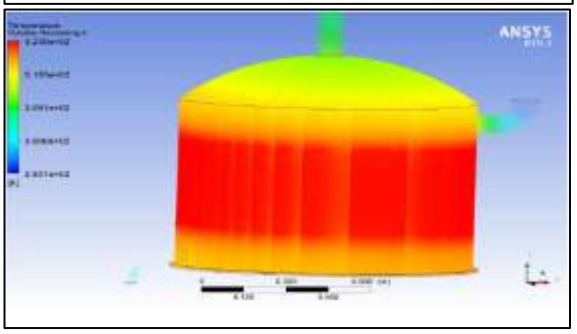

Figure 11. Temperature volume rendering

and higher around the wall of the digester. This is due to the variations in temperature in the helical coil heat exchanger. The heat transfer from the hot water in the helical coil to the waste food caused the input temperature to drop at the digester's inlet. In fixed dome digesters, the temperature dropped at the coil's output but rose in the waste food. Figure 10 illustrates how the temperature changes from red at the intake to blue at the end. This temperature was in the rendering volume of the fixed dome digester needed for the fermentation of wasted food in the fixed dome digester. As indicated in Figure 11, the temperature transferred from the hot water from the helical coil in the digester to couple with the waste food in the digester. The average temperature at the rendering volume of the temperature according to the color in the legend was 308.05K.

4. 5. Graphical Representation of Temperature Distribution

To validate the total temperature in the digester, Figure 12 shows the temperature distribution over the dome. Figure 13 indicates the temperature distribution along the x-axis by the plot of the line in the digester dome in the horizontal direction. The temperature varies in the dome and is constant at the center as indicated in the figure. Figure 13 shows the temperature distribution in the digester dome along the vertical axis to show the temperature in the digester by drawing the line in the digester from zero to some distance in the dome.

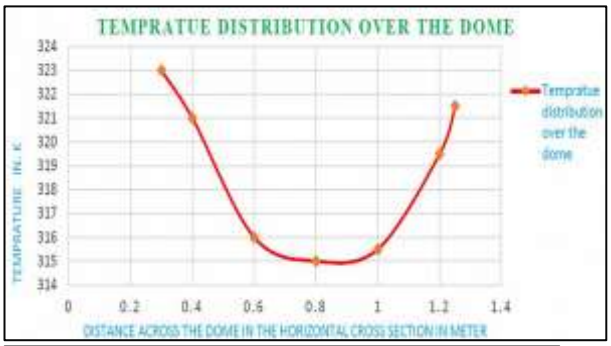

Figure 12. Temperature distribution over dome along the X- axis

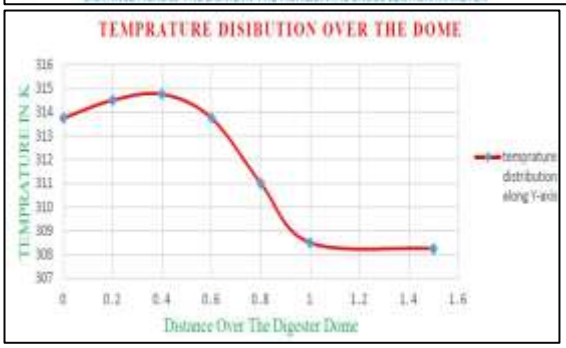

Figure 13. Temperature distributions over the dome along the Y-axis

5. Conclusions

This study focuses on the construction of a solar-heated biogas fermentation system paired with a thermal storage device for an ecologically friendly energy source by converting 1118 kg of food waste per day to biogas.

Jimma University's food waste was 1118 Kg/day and produced biogas of 44.7 m^3/day. According to the mathematical design, the digester runs for nine hours to meet the heat demands of fermentation, which total 18.4 m^3/day with two storage tanks of 7.7 m^3 capacity and a 43.5 m^3 volume of two fixed dome digesters. The detailed study was carried out in an average of the heat consumed by solar radiation by 2m^2 flat plate collectors and 122 collectors required to generate heat for the fermentation process. Thermal efficiency, pressure decrease, velocity of flow, and thermal output of solar collector heater systems with different mesh and flow types are all validated by CFD modeling. The turbulent flow and tiny mesh were optimized in this simulation. 333.2 K is the highest discharge water temperature. The efficiency of the flat plate collector was confirmed based on the output temperature. An anaerobic digester was subjected to a CFD simulation utilizing turbulent flow models.

Reference

1. McGrath, R. J.; & Mason, I. G. An observational method for the assessment of biogas production from an anaerobic waste stabilization pond treating farm dairy wastewater. Biosystems Engineering, (2004), 87(4), 471-478.

2. Hansen, T. L.; la Cour Jansen, J.; Davidsson, Å.; Christensen, T. H. Effects of pre-treatment technologies on quantity and quality of source-sorted municipal organic waste for biogas recovery. Waste Management, (2007), 27(3), 398-405.
3. Karellas, S.; Boukis, I.; Kontopoulos, G. Development of an investment decision tool for biogas production from agricultural waste. Renewable and Sustainable Energy Reviews, (2010), 14(4), 1273-1282.
4. Xydis, G.; Nanaki, E.; Koroneos, C. Exergy analysis of biogas production from a municipal solid waste landfill. Sustainable Energy Technologies and Assessments, (2013), 4, 20-28.
5. Jeihanipour, A.; Aslanzadeh, S.; Rajendran, K.; Balasubramanian, G.; Taherzadeh, M. J. High-rate biogas production from waste textiles using a two-stage process. Renewable Energy, (2013), 52, 128-135.
6. Lee, T. H.; Huang, S. R.; Chen, C. H. The experimental study on biogas power generation was enhanced by using waste heat to preheat inlet gases. Renewable energy, (2013), 50, 342-347.
7. Ngumah, C. C.; Ogbulie, J. N.; Orji, J. C.; Amadi, E. S. Biogas potential of organic waste in Nigeria. Journal of Urban and Environmental Engineering, (2013), 7(1), 110-116.
8. Ngumah, C.; Ogbulie, J.; Orji, J.; Amadi, E. Potential of organic waste for biogas and biofertilizer production in Nigeria. Environmental research, engineering and management, (2013), 63(1), 60-66.
9. Farid, MU.; Olbert, IA.; Bück, A.; Ghafoor, A.; Wu, G. CFD modelling and simulation of anaerobic digestion reactors for energy generation from organic wastes: A comprehensive review. Heliyon. (2025), 11, e41911.
10. Panchenko, VA.; Kovalev, AA. ; Kovalev, DA. ; Litty, YV. Review of modern methods and technologies for using of solar energy in the operation of anaerobic digestion systems. International Journal of Hydrogen Energy. (2023), 48(53), 20264-78.
11. Rodríguez-Jiménez, LM. ; Pérez-Vidal, A.; Torres-Lozada P. Research trends and strategies for the improvement of anaerobic digestion of food waste in psychrophilic temperature conditions. Heliyon. (2022), 1, 8(10), e11174.
12. Servati, P.; Hajinezhad, A, CFD simulation of anaerobic digester to investigate sludge rheology and biogas production. Biomass Conversion and Biorefinery, (2020), 10(4), 885-99.
13. Chen, J.; Chen. ; A. Shaw, J.; Yeh, C.; Chen, S. CFD simulation of two-phase flows in anaerobic digester. In Journal of Physics: Conference Series. IOP Publishing. (2019), 1300 (1), 012048.
14. Li, L.; Wang, K.; Wei, L.; Zhao, Q.; Zhou, H.; Jiang, J. CFD simulation and performance evaluation of gas mixing during high solids anaerobic digestion of food waste. Biochemical Engineering Journal. (2022), 178:108279.
15. Dabiri, S.; Noorpoor, A.; Arfaee, M.; Kumar, P.; Rauch, W. CFD Modeling of a stirred anaerobic digestion tank for evaluating energy consumption through mixing. Water. (2021), 13 (12), 1629.
16. Li, J.; Wan, D.; Jin, S.; Ren, H.; Gong, S.; Novakovic, V. Feasibility of annual wet anaerobic digestion temperature-controlled by solar energy in cold areas. Applied Thermal Engineering. (2023), 25, 219:119333.
17. Dewangan, M.; Mishra, S. S. Determination of Shape Factor of Fixed Dome and Spherical Shape of Biogas Digester by Method of Thermal Simulation. International Journal of Science and Research, (2016), 5 (8).
18. Asmare, M. Design of cylindrical fixed dome biodigester in the condominium houses for cooking purposes at Dibiza Site, East Gojjam, Ethiopia. American Journal of Energy Engineering, (2014), 2(1), 16-22.
19. Tadesse, M.; Adamu, M. Design and development of biogas production system from waste coffee pulp and its wastewater around Tepi. Int. J. Recent Dev. Eng. Technol, (2017), 6, 18-30.
20. Alemu, D. Optimal design of solar water heating systems. Zede Journal, (1998), 15, 53-60.

21. Mohammadrezaei, R.; Zareei, S.; Behroozi-Khazaei, N. Improving the performance of mechanical stirring in biogas plant by computational fluid dynamics (CFD). Agricultural Engineering International. CIGR Journal, (2017), 19(4), 91-97.